Considerations for Source Pulses and Antennas in UWB Radio Systems

Zhi Ning Chen, *Member, IEEE*, Xuan Hui Wu, *Student Member, IEEE*, Hui Feng Li, *Student Member, IEEE*, Ning Yang, and Michael Yan Wah Chia, *Member, IEEE*

***Abstract*—This paper addresses two vital design considerations in ultrawide-band radio systems. One is that radiated power density spectrum shaping must comply with certain emission limit mask for coexistence with other electronic systems. Another is that the design of source pulses and transmitting/receiving antennas should be optimal for the performance of overall systems. The design of source pulses and transmitting/receiving antennas under the two considerations is discussed. First, the characteristics of transmitting/receiving antenna systems are described by a system transfer function. Then, the design of source pulses and transmitting antennas are studied based on the considerations for emission limits. Finally, the design of transmitting and receiving antennas are investigated in terms of pulse fidelity and system transmission efficiency. In the studies, thin wire dipoles with narrow bandwidths and planar dipoles with broad bandwidths are exemplified.**

***Index Terms*—Broad-band antennas, pulsed antennas, ultra-wide-band antennas (UWB).**

I. Introduction

SINCE the 1970s, ultrawide-band (UWB) technology has widely been investigated and developed for wireless communication applications [1]–[5]. Recently, much effort has been devoted to commercial short-range UWB systems.

Radio systems based on UWB technology offer opportunities for high resolution radar imaging, rejection of multipath cancellation effect, transmission of high data rate signals, coding for security and low probability of intercept, especially in multiuser network applications [6]–[9]. In general, UWB radio systems transmit and receive temporally short pulses without carriers or modulated short pulses with carriers.

On the one hand, carrier-free UWB radio systems usually employ very short pulses in the order of subnanosecond (ns) or occupy an extremely broad bandwidth typically larger than 20% or 500 MHz. Such systems are capable of providing low system complexity and low costs because of their direct transmission and reception of pulsed signals and the least RF devices in their front-ends as against conventional narrow-band radio systems.

On the other hand, the carrier-free or carrier UWB radio systems may possibly interfere with existing electronic systems since short pulses or modulated pulses occupy extremely wide spectra, which cover many bands being used. Due to potential interference, the Federal Communication Commission (FCC) regulated the emission limits for the allocated 7.5-GHz bandwidth (3.1–10.6 GHz, termed the UWB band in this paper) for unlicensed use of commercial UWB communication devices (termed UWB systems in this paper). The emission limits will be crucial considerations for the design of source pulses and antennas in UWB systems. The study will show that the radiated power density spectrum (PDS) shaping can be controlled by selecting source pulses and tailored by designing transmitting antennas.

Moreover, the emission limits indicate that UWB systems may operate across a 7.5 GHz or a 110% 10-dB fractional bandwidth with very low radiated power. Due to the extremely wide operating bandwidth, the transmission and reception of signals in UWB systems are distinct from conventional narrow-band systems. First, the design of source pulses significantly affects the performance of the UWB system. Properly selecting the source pulse can maximize the radiated power within the UWB band and meet the required emission limits without any filters before transmitting antennas. Secondly, the waveforms of the pulses arriving at a receiver usually do not resemble the waveforms of its source pulses at a transmitter. The transmitting/receiving antennas with frequency-dependant transfer response act as temporal differentiators/integrators or spectral/spatial filters. As a result, the selection of a template for correlation detection at a receiver strongly depends on the characteristics of both source pulses and transmitting/receiving antennas. Thirdly, the antennas should be analyzed and modeled in both time domain (TD) and frequency domain (FD) or a TD [10]–[13]. Fourthly, the assessment and the design of the antennas should be carried out from an overall system point of view not only an individual antenna element [14]–[20].

In this paper, we emphasize two essential and special design considerations in UWB systems. One is that radiated PDS shaping must conform to certain emission limit masks for the reduction of possible interference with other electronic systems. Another is that the design of source pulses and transmitting/receiving antennas should be optimized for the performance of overall systems, such as maximum ratio of signal to noise (S/N) or minimal bit-error-rate (BER). The following discussion is carried out under such considerations for both single-band and multiband schemes.

First, a frequency-dependent transmission equation based on the Friis transmission formula is employed to describe transmitting/receiving antenna systems. Then, the design of source pulses and transmitting antennas are studied and

Manuscript received February 6, 2003; revised August 7, 2003.

The authors are with the Institute for Infocomm Research (I^2R), Agency of Science Technology And Research (ASTAR), Singapore 117674, Singapore (chenzn@i2r.a-star.edu.sg).

Digital Object Identifier 10.1109/TAP.2004.831405

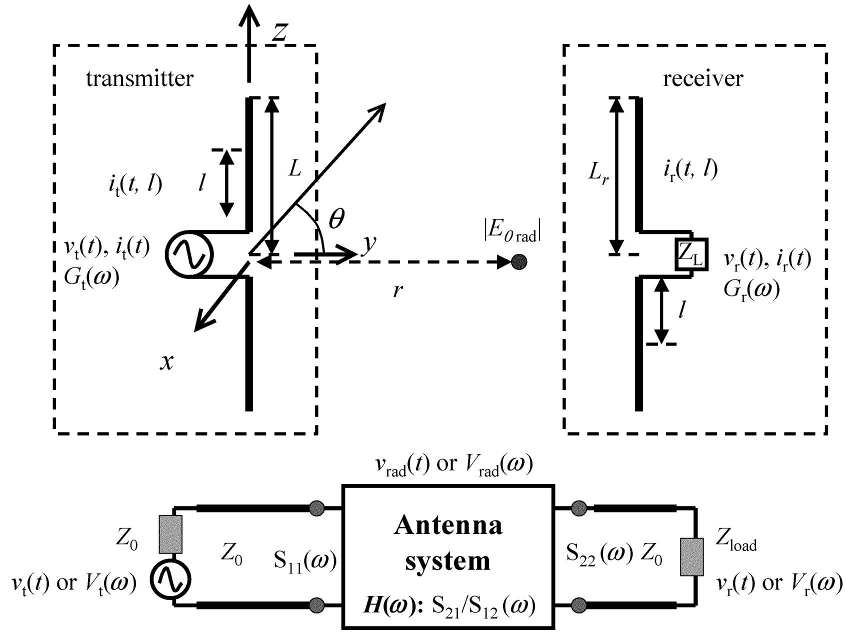

Fig. 1. Schematic diagram of an antenna system in UWB radio systems.

optimized under the considerations for emission limits. At last, transmitting/receiving antenna systems are assessed by pulse fidelity and system transmission efficiency. Thin wire dipoles with narrow bandwidths and planar dipoles with broad bandwidths are exemplified in the discussion. The numerical TD and FD methods used in the studies include a finite-difference time-domain (FDTD) method, a time-domain integration equation (TDIE) method, and the method of moments (MoM).

II. Description of Antenna Systems

Consider a typical transmitting/receiving antenna system in UWB radio systems as shown in Fig. 1. The Friis transmission formula relates the output power of the receiving antenna to the input power of the transmitting antenna as shown in (1). It is assumed that each antenna is in the far field of the other

$$\frac{P_r}{P_t} = \left(1-|\Gamma_t|^2\right)\left(1-|\Gamma_r|^2\right) G_r G_t |\hat{\rho}_t \cdot \hat{\rho}_r|^2 \left(\frac{\lambda}{4\pi r}\right)^2 \quad (1)$$

where P_t, P_r: time average input power of the transmitting antenna and time average output power of the receiving antenna; Γ_t, Γ_r: return loss at the input of the transmitting antenna and the output of receiving antenna; G_t, G_r: gain of the transmitting antenna and the receiving antenna; $|\hat{\rho}_t \cdot \hat{\rho}_r|^2$: polarization matching factor between the transmitting antenna and the output of receiving antenna; λ: operating wavelength; and r:distance between antennas.

In this formula, the gain of the transmitting antenna and receiving antenna, G_t and G_r are the functions of orientation (θ, ϕ). In particular, this formula is available at a specific operating wavelength, λ or frequency. It is still correct for narrow-band systems because usually, all the parameters in formula (1) hardly vary within operating frequency ranges. However, it is clear that the UWB system response between transmitting and receiving antennas is frequency-dependant. The formula can be rewritten as follows:

$$\frac{P_r(\omega)}{P_t(\omega)} = \left(1-|\Gamma_t(\omega)|^2\right)\left(1-|\Gamma_r(\omega)|^2\right) \times G_r(\omega) G_t(\omega) \left|\hat{\rho}_t(\omega) \cdot \hat{\rho}_r(\omega)\right|^2 \left(\frac{\lambda}{4\pi r}\right)^2. \quad (2)$$

If we define a transfer function $H(\omega)$ to describe the relation between the source and output signal (voltage) $[V_t(\omega)/2]^2/2[= P_t(\omega)Z_0]$ and $V_r^2(\omega)/2[= P_r(\omega)Z_{\mathrm{load}}]$ the formula can be simplified as follows:

$$\begin{aligned} H(\omega) &= \frac{V_r(\omega)}{V_t(\omega)} = \left|\sqrt{\frac{P_r(\omega)}{P_t(\omega)}\frac{Z_{\mathrm{load}}}{4Z_0}}\right| e^{-j\phi(\omega)} \\ &= |H(\omega)|\, e^{-j\phi(\omega)} \\ \phi(\omega) &= \phi_t(\omega) + \phi_r(\omega) + \frac{\omega r}{c}. \end{aligned} \quad (3)$$

In (3), c denotes velocity of light, and $\phi_t(\omega)$ and $\phi_r(\omega)$ are, respectively, the phase variation due to the transmitting and receiving antennas. Clearly, the transfer function is determined by the characteristics of transmitting and receiving antennas, such as impedance matching, gain, polarization matching, the distance between the antennas as well as the orientation of the antennas if the effect of a RF channel is ignored. Therefore, the transfer function $H(\omega)$ can be used to describe general antenna systems, which may be dispersive.

Also, we can consider the antenna system as a two-port network. Therefore, the transfer function can be measured in terms of S_{12} or S_{21} when the source impedance and loading are matching. It suggests from (2) and (3) that the measurable parameter S_{12} or $H(\omega)$ integrates all of the important system performance, such as gain, impedance matching, polarization

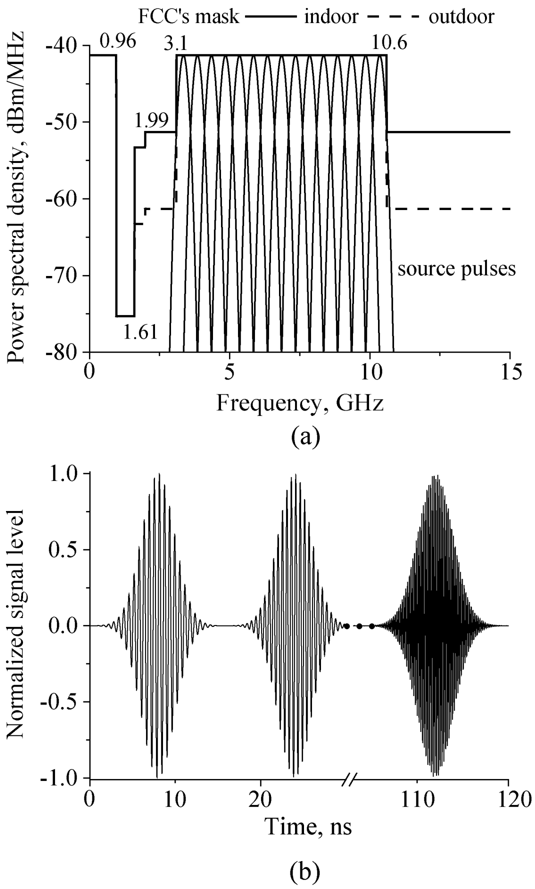

Fig. 2. Multiband scheme (a) PDS with an emission limit mask by FCC and (b) waveforms in time domain.

matching, path loss, and phase delay. Therefore, it can be used to assess the performance of antenna systems.

Similarly, the relation between the radiated electric fields (pulses) and source pulses at the transmitting antenna can be expressed in the following:

$$\begin{aligned}\vec{E}_{\rm rad}(\omega) &= \vec{H}_{\rm rad}(\omega)V_t(\omega)\\ &= \hat{a}\left|H_{\rm rad}(\omega)\right| e^{-j\phi_{rad}(\omega)}V_t(\omega);\\ \phi_{\rm rad}(\omega) &= \phi_t(\omega)+\frac{\omega r}{c}.\end{aligned} \tag{4}$$

Certainly, the transfer function $\vec{H}_{\rm rad}(\omega)$ is a vector with the direction determined by the polarization direction $\hat{a}$ of the transmitting antenna and is determined by the characteristics of the transmitting antenna, such as impedance matching, gain, and the orientation of observation point. $V_t(\omega)$ is the spectrum of a source signal (voltage). Also, this transfer function can be used to evaluate the radiated PDS for the considerations for emission limits.

III. System Schemes and Emission Limits

The emission limits mask regulates the spectra of, for example, 3.1–10.6 GHz by FCC, and effective isotropic radiated power (EIRP) levels within the spectra. In practice, UWB systems can utilize the UWB band in a variety of ways. For instance, multiband (single carrier/multicarrier) and single-band schemes have been proposed for UWB radio systems. Here, the investigation will show that to comply with the emission limits, the design considerations for source pulses and transmitting antennas are subject to the specific system schemes.

A. Multiband Scheme

The available UWB band can be divided into several subbands. Each of source pulses is shaped to occupy only one subband. For example, Fig. 2(a) reveals the scheme of 15 uniform subbands for 7.5-GHz UWB band, where the 10-dB bandwidths are of 500 MHz. Fig. 2(b) displays a Gaussian pulse $v_0(t)=e^{-(t/\sigma)^2}$ with $\sigma = 1366$ ps, which is modulated by the sine signals with the frequencies of $(3.35+n\times 0.5)$ GHz $(n=0,1,2,\ldots,14)$. It is clear that possible interference with other systems outside the UWB band and between the subbands can be suppressed if the pulse parameter σ and the modulation frequencies are properly set. Another advantage of this scheme is to avoid possible interference appearing within the UWB band because it allows UWB system users to suspend any subband, within which the interference with other systems becomes severe. For example, the transmission of the pulse covering the subband of 5.6–6.1 GHz will halt when the UWB systems have a strong interference with W-LAN users (IEEE 802.11 upper band). Consequently, this scheme is good for interference considerations but greatly increases the complexity of system design.

B. Single-Band Scheme

Alternatively, the single-band scheme is proposed for simplifying system design. The single source pulse, which usually has a very short duration, is shaped so that its spectrum occupies as wide as possible band within the UWB band for high data rates and S/N. From (4), it is manifest that there are at least two ways to meet the emission limit mask. One is to control the spectra, $V_t(\omega)$ of source signals directly when the transfer function, $\vec{H}_{\rm rad}(\omega)$ keeps unchanged within the UWB band. Another is to tailor the spectra, $V_t(\omega)$ of source signals by means of the filtering function of $\vec{H}_{\rm rad}(\omega)$, viz. to control $\vec{H}_{\rm rad}(\omega)V_t(\omega)$ when $V_t(\omega)$ does not meet the emission limits mask.

The first method also involves two scenarios with 10-dB bandwidths narrower than the UWB band. One is that the 10-dB bandwidth fully falls into the UWB band by properly selecting source pulses. Otherwise, the 10-dB bandwidth spectrum of the pulse can also be shifted into the UWB band by modulating the pulse with a proper sine carrier. Both cases will make antenna design easy.

In the second method, the transmitting antenna acts as a radiator with a special filtering transfer function, which is designed as a filter to suppress the unwanted radiation outside the UWB band or in the specific band. It is usually difficult to achieve it in antenna designs.

Here, the discussion focuses on the selection of source pulses for the emission control consideration first, assuming that the bandwidth of a transmitting antenna is broad enough so that within the UWB band $\vec{H}_{\rm rad}(\omega)$ is constant. In principle, all the pulses with the spectra (wider than 500 MHz stipulated by FCC) falling into the UWB band can be used as the signals. However, for practical purposes, only are the pulses, which are easily generated, controlled, and low power-consumption (no direct component), selected to generate UWB signals.

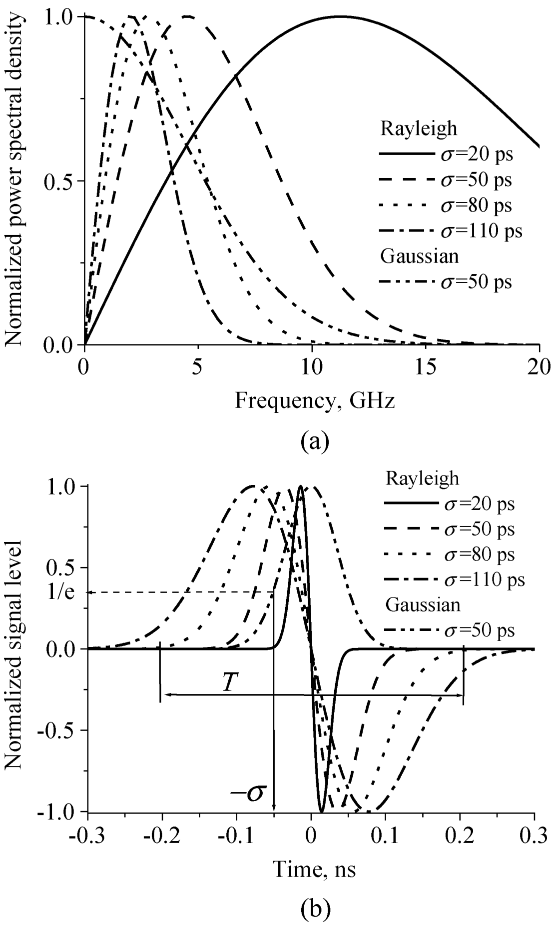

Fig. 3. Single-band scheme (with Gaussian and Rayleigh pulses in (a) PDS and (b) waveforms in time domain.

Due to unique temporal and spectral properties, a family of Rayleigh (differentiated Gaussian) pulses, $v_n(t)$ or $\widetilde{v}_n(\omega)$ is widely used as the source pulses in UWB systems

$$v_n(t) = \frac{d^n}{d^n t}\left[e^{-\left(\frac{t}{\sigma}\right)^2}\right]; \quad \widetilde{v}_n(\omega) = (\mathrm{j}\omega)^n \sigma\sqrt{\pi} e^{-\left(\frac{\omega\sigma}{2}\right)^2} \quad (5)$$

where, the pulse parameter σ stands for the time when Gaussian pulse $v_0(\sigma) = e^{-1}$. The pulse duration T is defined as the interval between the start and the end of the pulse where the values $|v_n(t = \pm T/2)|$ decreases from the normalized peak value to e^{-9} as shown in Fig. 3. Fig. 3 displays the pulses $v_0(t)$ and $v_1(t)$. Obviously, only is the $v_1(t)$ a monocycle pulse, which is easily generated by RF circuits and does not generate any direct currents (DC) component in the FD.

The calculation shows that the first-order Rayleigh pulses with $\sigma > 61$ ps ($T > 305$ ps) occupy the spectra of 10-dB bandwidths of <7.5 GHz as shown in Fig. 3(a). However, their spectra do not fully fall into the UWB band defined by the FCC. As mentioned above, they can completely be moved into the UWB band to meet the FCC's emission limits if they are modulated by sine signals with proper frequencies.

The calculation also demonstrates that some of higher-order Rayleigh pulses can match the UWB band directly such as the fourth-order Rayleigh pulses with $67\ \mathrm{ps} < \sigma < 76$ ps, the fifth-order Rayleigh pulses with $72\ \mathrm{ps} < \sigma < 91$ ps, and the sixth-order Rayleigh pulses with $76\ \mathrm{ps} < \sigma < 106\ \mathrm{ps}$.

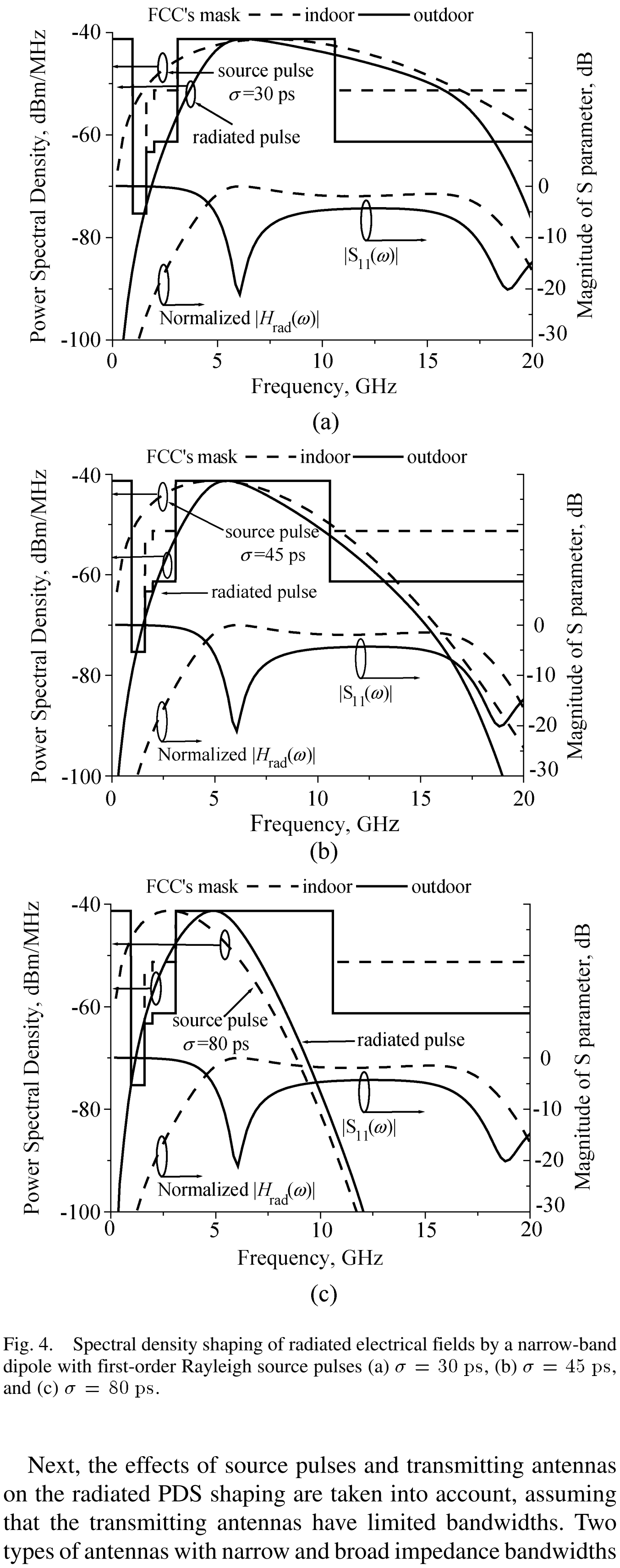

Fig. 4. Spectral density shaping of radiated electrical fields by a narrow-band dipole with first-order Rayleigh source pulses (a) $\sigma = 30$ ps, (b) $\sigma = 45$ ps, and (c) $\sigma = 80$ ps.

Next, the effects of source pulses and transmitting antennas on the radiated PDS shaping are taken into account, assuming that the transmitting antennas have limited bandwidths. Two types of antennas with narrow and broad impedance bandwidths are exemplified.

The typical center-fed thin-wire dipole antennas with narrow bandwidths are first discussed. The thin-wire straight dipole of $L = 11$ mm in length and having a 0.3-mm radius was numerically simulated using the time-domain integration equation

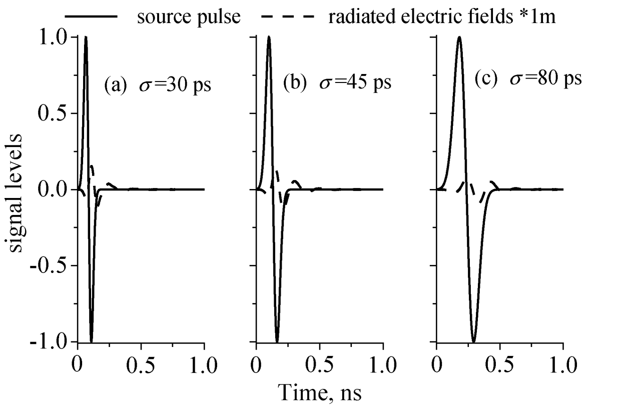

Fig. 5. Comparison of waveforms of source pulses and the radiated electrical fields ($^*1\mathrm{m}$) (a) $\sigma = 30$ ps; (b) $\sigma = 45$ ps; and (c) $\sigma = 80$ ps.

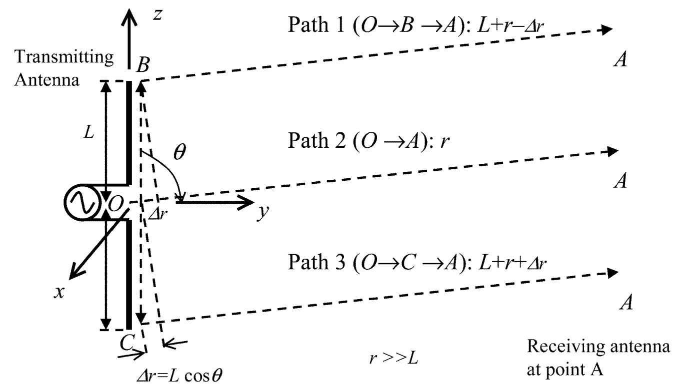

Fig. 6. Multipath model for a transmitting antenna.

(TDIE) method. The well-matched frequency is 5.85 GHz with a 10-dB bandwidth of 25% ($|S_{11}|$) as shown in Fig. 4. The normalized radiated transfer function $|\vec{H}_{\mathrm{rad}}(\omega)|$ is also illustrated in Fig. 4. In the study, three typical first-order Rayleigh pulses with $\sigma = 30$, 45, and 80 ps are used as source pulses. The radiated fields are the copolarization components $|E_{\theta\mathrm{rad}}|$ in the direction of $\theta = 90°$ and at a distance of $r = 1960$ mm as shown in Fig. 1. The comparison between the spectra of source and radiated pulses normalized to -41.3 dBm/MHz is depicted in Fig. 4. From the transfer function $|H_{\mathrm{rad}}(\omega)|$ shown in Fig. 4, it is readily observed that the dipole acts as a high-pass filter within the UWB band. Thus, the tailored radiated spectrum of the short pulse cannot fully meet the emission limit mask when the pulse has the high emission levels at the frequencies higher than 10.6 GHz as shown in Fig. 4(a). In contrast, Fig. 4(c) displays that the radiated spectrum of the longest pulse also does not meet the emission limit mask because of its high emission levels at the frequencies lower than 3.1 GHz. Fig. 4(b) evidently demonstrates that the radiated spectrum can completely comply with the specific emission constraint mask by properly selected source pulses for a given transmitting antenna. Another important parameter, the efficiency of the transmitting antenna can be evaluated in the following:

$$\eta_{\mathrm{rad}} = \frac{\int_0^\infty P_{\mathrm{t}}(\omega)\left(1-|S_{11}(\omega)|^2\right)d\omega}{\int_0^\infty P_{\mathrm{t}}(\omega)d\omega} \times 100\%. \tag{6}$$

Both source pulse and transmitting antenna determine the efficiency η_{rad}. The calculated efficiency η_{rad} is about 53% for the case shown in Fig. 4(b), where the spectrum well conforms to the emission limit mask.

Fig. 5 further displays the waveforms of the radiated electric fields with $\sigma = 30$, 45, and 80 ps or $\sigma_{\mathrm{ant}}/\sigma = 1.22$, 0.82, and 0.46. The parameter $\sigma_{\mathrm{ant}} = L/c$ indicates the time for light to travel the length, L of the antenna arm at the velocity $c = 3 \times 10^8$ m/s. Fig. 5 shows the distorted waveforms of the radiated pulses due to the highpass filtering of the antennas in the FD [21]. In the TD, the distorted waveforms of the radiated pulses basically attribute to the reflection appearing at the ends (including the input) of the dipole. The pulses radiated from the ends of the dipole, namely Point O, B, and C arrive at the receiving antenna located at Point A (in far-field zone) through the paths of different lengths, namely Path 1, 2, and 3 as illustrated in Fig. 6. The length difference between the paths also causes the time delay in the TD or the phase difference in the FD.

As an example, the effect of impedance matching between source and input of an antenna on the waveforms of the radiated pulses is described in the FD. As known, the relation between input current $I(\omega)$, voltage $U(\omega)$, and impedance $Z(\omega)$ of a dipole is

$$I(\omega) = \frac{U(\omega)}{Z(\omega)}. \tag{7}$$

The corresponding inverse Fourier Transform is

$$\begin{aligned} i(t) &= F^{-1}[I(\omega)] = F^{-1}\left[\frac{U(\omega)}{\mathrm{Z}(\omega)}\right] \\ &= \begin{cases} F^{-1}[j\omega C U(\omega)] \cong C\frac{dU(t)}{dt}, & \mathrm{Z}(\omega) \cong -\frac{j}{\omega C} \\ & \text{for } L \ll \lambda \\ F^{-1}\left[\frac{U(\omega)}{R}\right] = \frac{U(t)}{R}, & \mathrm{Z}(\omega) = R \\ F^{-1}\left[\frac{U(\omega)}{\mathrm{Z}(\omega)}\right], & \text{otherwise.} \end{cases} \end{aligned} \tag{8}$$

It is clear that the waveform of the input current is related to frequency-dependent input impedance of the dipole. For $\sigma_{\mathrm{ant}}/\sigma \ll 1 (L \ll \lambda)$, the input current $i(t)$ is roughly the first-order differential of input voltage $U(t)$ because the input impedance of a short dipole approximates pure capacitance. For broad-band well-matched cases, the input current $i(t)$ is of the same waveform as the input voltage $U(t)$. For other cases, the input current $i(t)$ may have different waveform from the input voltage $U(t)$ due to the reflection at the dipole input. As known, the varied current waveform on the dipole certainly radiates the different pulse waveforms from the original source pulse.

Then, a broad-band planar dipole is considered for comparison with the aforementioned narrow-band thin-wire dipole. In this design two 18 × 18-mm planar radiators are used to replace the thin wire radiators shown in Fig. 1 and positioned face-to-face [22].

For comparison purpose, the same source pulses as those used in Fig. 4 are applied to the input of the transmitting dipole. The observed fields are the copolarization components $|E_{\theta\mathrm{rad}}|$ in the direction of $\theta = 90°$ and at the distance of $r = 1960$ mm as shown in Fig. 1. Fig. 7 shows the power density spectra of the radiated pulses, the transfer function, and return loss $|S_{11}|$. It is readily seen that all the radiated power density spectra cannot comply with the FCC's emission constraint mask well

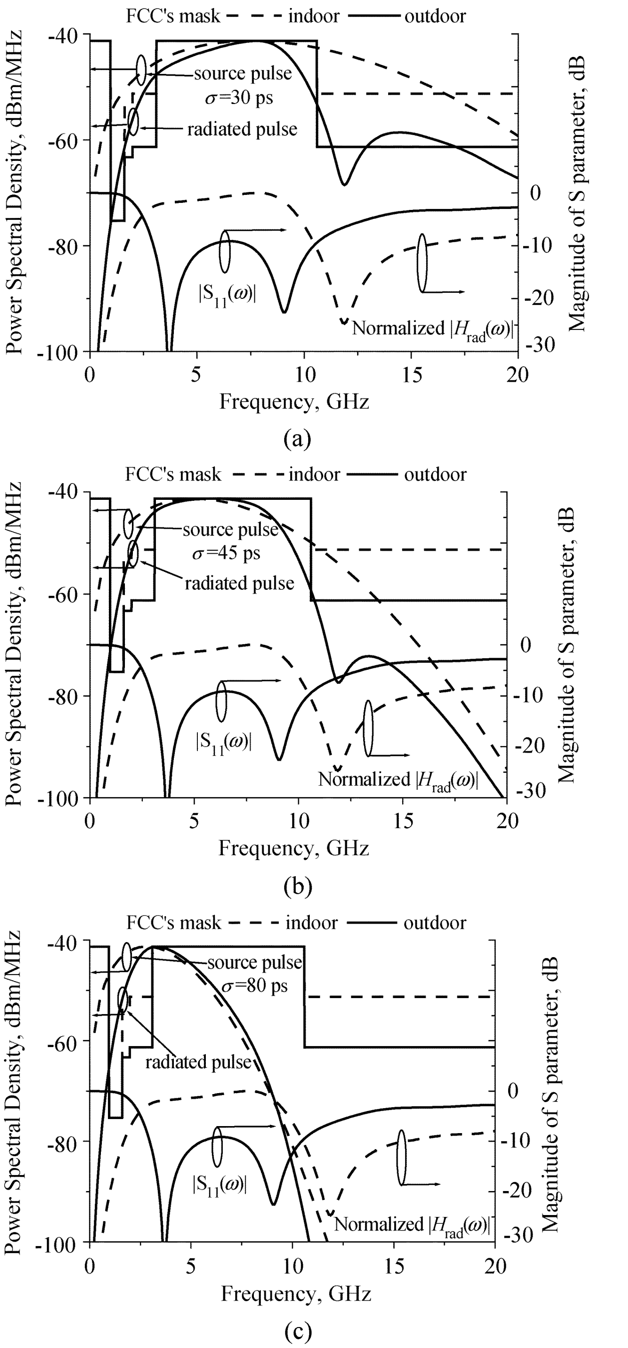

Fig. 7. Spectral density shaping of radiated electrical fields by a broad-band dipole with first-order Rayleigh source pulses (a) $\sigma = 30$ ps, (b) $\sigma = 45$ ps, and (c) $\sigma = 80$ ps.

because the broad-band dipole acting as an allpass filter with a flat transfer function $|\vec{H}_{\rm rad}(\omega)|$ hardly tailors the spectra across a bandwidth wider than the UWB band. As mentioned above, the broad-band designs are suitable for the scenarios, where the spectra of the source pulses conform to FCC's emission limit masks themselves, such as the multiband scheme.

IV. Transmitting/Receiving Antenna System

Another crucial criterion of the UWB antennas is associated to the performance of overall transmitting/receiving antenna systems. This consideration stems from the fact that compared

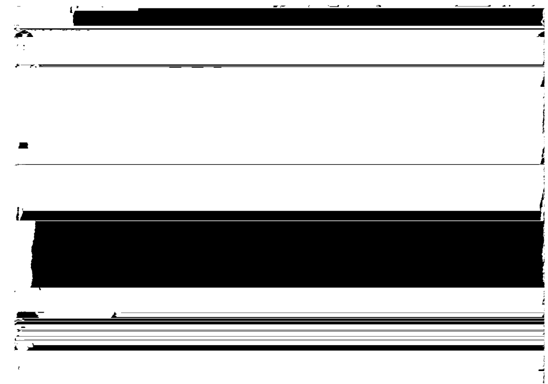

Fig. 8. Magnitude of system transfer function $H(\omega)$ and radiated transfer function $H(\omega)^*1\mathrm{m}$ for narrow-band and broad-band antenna systems.

with antennas in narrow-band radio systems, antennas or antenna systems in the UWB systems hardly maintain invariable performance across a range of a few gigahertz. The variation in the performance of the antennas or antenna systems significantly affects the waveforms and spectra of the radiated pulses as discussed above. As a result, the waveforms of the pulses received by a receiver are different from those of the source pulses applied at the input of a transmitting antenna (especially for the single-band scheme) and even distort severely. Furthermore, the transfer function can be used to assess the performance of antenna systems and determine the templates at a receiver. However, it is difficult to exactly formulate the transfer function between arbitrary transmitting/receiving antennas in a close form due to the complicated frequency-dependent features of the antennas [11]–[13]. Therefore, the effects of the transfer function $H(\omega)$ given in formula (3) on the output pulses are investigated numerically. Also, the performance of antenna systems is measured in terms of pulse fidelity and system transmission efficiency.

The received pulses, which are transmitted through both narrow-band and broad-band antenna systems, are compared for single-band and multiband schemes. For the single-band and multiband schemes, the source pulses used in Fig. 4 and Fig. 2 are adopted, respectively, where the voltage source has a 100-Ω inner impedance. The narrow-band and broad-band antenna systems comprise two thin-wire and planar square dipoles which have been used in Fig. 4 and 7, respectively. The receiving antennas have the 100-Ω loading. The distance between the transmitting and receiving dipoles are 1960 mm. The receiving antennas are oriented to receive the copolarization components $|E_{\theta\rm rad}|$ radiated by the transmitting dipoles at the direction of $\theta = 90°$ and $\phi = 90°$ as shown in Fig. 1.

Fig. 8 illustrates the system transfer function $|H(\omega)|$ and the radiation transfer function $|H_{\rm rad}(\omega)|$ for the narrow-band and broad-band antenna systems. The comparison exhibits that the broad-band antenna system features a $|H(\omega)|$ or $|H_{\rm rad}(\omega)|$ flatter than the narrow-band antenna system within the UWB band.

Fig. 9 shows the waveforms of the received pulses in the single-band and multiband schemes, which go through a narrow-band antenna system (a pair of thin-wire dipole). Clearly, the pulse waveforms illustrated in Fig. 9(a) and (b) are not identical with the waveforms of source pulses even the

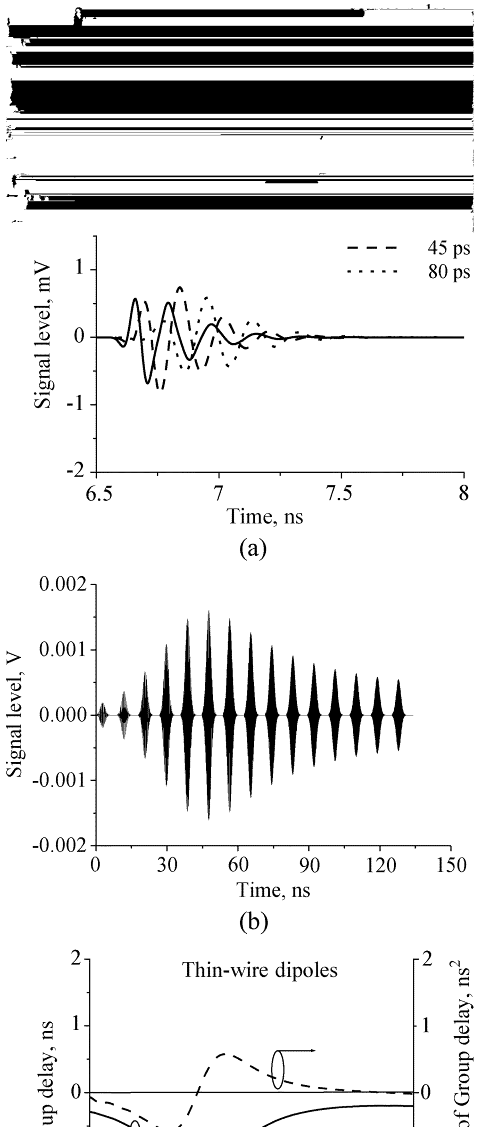

Fig. 9. (a) Waveforms of received pulses in a single-band scheme, (b) waveforms of received pulses in a multiband scheme, (c) group delay and its variation of $H(\omega)$ for a narrow-band antenna system.

radiated pulses shown in Fig. 5. In the single-band scheme, the severe distortion results mainly from the narrow-band filtering of the antenna systems. In other words, the dispersion in magnitude and phase of $H(\omega)$ results in the distortion of the pulse waveforms. In a multiband scheme, the change in the magnitude of $H(\omega)$ causes the uneven envelop of the magnitudes of the received signals, which envelop accords with the shape of magnitude of $H(\omega)$ shown in Fig. 8. The unequal amplitudes of the signals result in the different S/N in the subbands.

Fig. 9(c) displays the group delay and the variation in the group delay, which are also the factor to distort the signals, especially when the large change in the group delay occurs. This differentiates the design considerations for UWB antenna systems from narrow-band antenna systems. Due to narrow-band operation, the latter usually has linear phase response across the operating band. The important influence of the group delay leads to the shift in carriers. That means that the maximum energy can be detected at the different frequency from the original carrier.

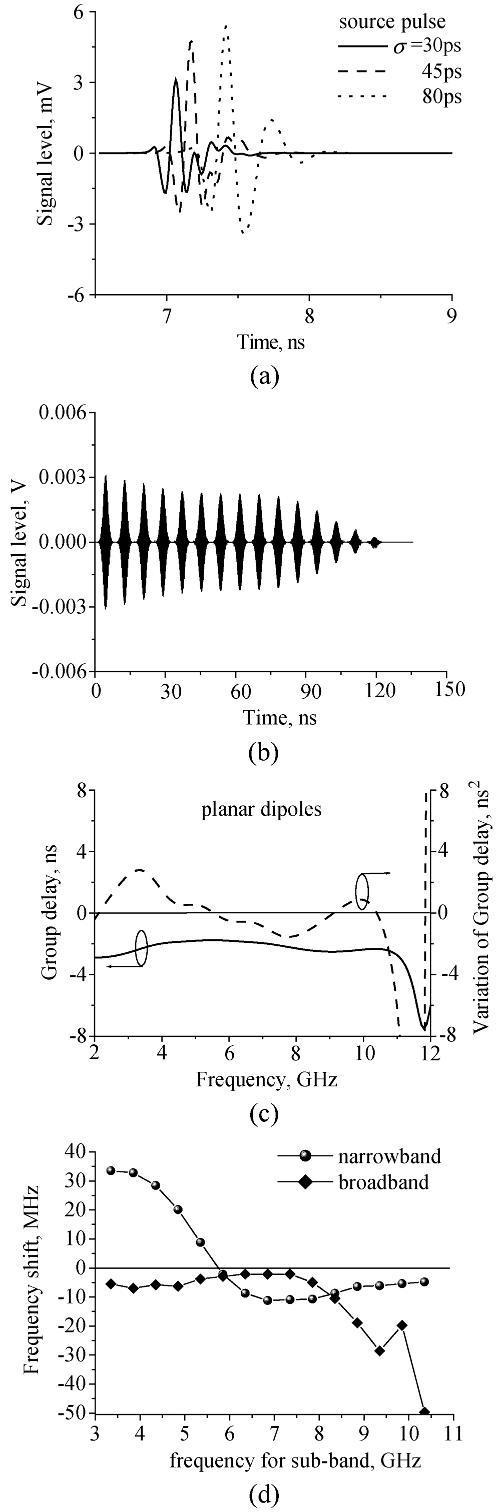

Fig. 10. (a) Waveforms of received pulses in a single-band scheme, (b) waveforms of received pulses in a multiband scheme, (c) group delay and its variation of $H(\omega)$ for a broad-band antenna system, (d) frequency shift in terms of maximum fidelity at the varied detecting frequencies.

Similarly, a broad-band antenna system (a pair of planar dipole) is used to transmit and receive the pulses. The waveforms of the received pulses in the single-band and multiband schemes are illustrated in Fig. 10. Compared with the pulse waveforms illustrated in Fig. 9(a) and (b), the pulse waveforms shown in Fig. 10(a) and (b) change less. The pulse waveforms in the single-band scheme are similar to the second Rayleigh pulses. The longer the pulse is, the larger the time delay is. This turns out the fact that in the TD the reflection occurring at the ends of the dipoles essentially brings on the distortion of the waveforms although the source is well matched to the input of the antenna within a broad bandwidth. Because of the flat magnitude response of $|H(\omega)|$, the envelop of the pulse magnitudes in the multiband scheme are more even than that shown in Fig. 9(b), which also agrees with the shape of the magnitude $|H(\omega)|$ shown in Fig. 8. However, it should be noted that the group delay and the variation of the group delay depicted in Fig. 10(c) are greater than those shown in Fig. 9(c) since the former planar dipoles have larger size than the latter thin-wire dipoles. The work by Hertel and Smith in 2003 has proven that the group delay can significantly contribute to the distortion of the radiated pulses although the magnitude of the antenna response is very flat [23].

Fig. 10(d) demonstrates the frequency shift of each modulated pulses with respect to the 15 carriers. The curves of the frequency shift are closely related to the system response displayed in Fig. 8. It manifestly suggests that in the multiband scheme the pulses be primarily affected by the magnitude of the system response because the group delay varies slightly within one width-limited subband.

To evaluate the transmitting and receiving capability of the antenna systems, viz., one of crucial parameters of antenna systems, Formula (2) is rewritten as follows:

$$\begin{aligned} 10\log\left(\frac{P_r(\omega)}{P_t(\omega)}\right) &= 10\log\Big[\left(1-|\Gamma_t(\omega)|^2\right)\left(1-|\Gamma_r(\omega)|^2\right) \\ &\qquad \times G_r(\omega)G_t(\omega)\left|\hat{\rho}_t(\omega)\cdot\hat{\rho}_r(\omega)\right|^2\left(\frac{\lambda^2}{4\pi}\right)\Big] \\ &\quad - 10\log(4\pi r^2) \\ &= \eta(\mathrm{dB}) - 10\log(4\pi r^2) \end{aligned} \tag{9}$$

where, the first term is independent of the distance between transmitting and receiving antennas and indicates the transmitting and receiving capability of antenna systems. Fig. 11 shows the transmitting and receiving capability of antenna systems for the abovementioned narrow-band and broad-band antenna systems. For both single-band and multiband schemes the broad-band antenna system always transmits and receives the pulses much more efficiently than the narrow-band antenna system. Fig. 11(a) further suggests that for a given antenna system in a single-band scheme the system efficiency be also dependant on the pulse widths. Moreover, Fig. 11(b) points out that the efficiency of a given antenna system varies with the carriers applied to a multiband scheme.

Furthermore, the fidelity of the signal of an antenna system is calculated to assess the quality of a received pulse and select a proper detection template, [10]. The definition of the fidelity can be written in

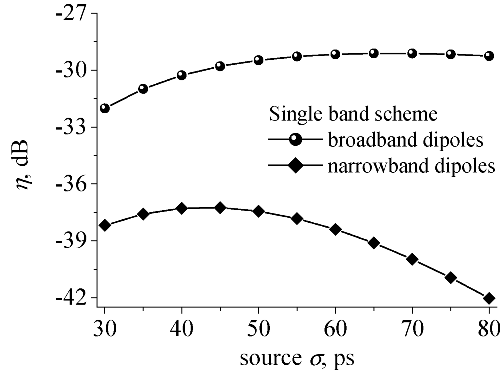

(a)

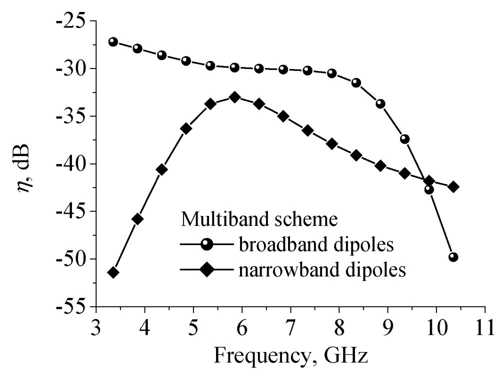

(b)

Fig. 11. System transmission efficiency (a) single-band scheme and (b) multiband scheme.

$$F = \max_{\tau} \int_{-\infty}^{\infty} L\left[p_{\mathrm{source}}(t)\right] p_{\mathrm{output}}(t-\tau)dt \tag{10}$$

where, the source pulse $p_{\mathrm{source}}(t)$ and output pulse $p_{\mathrm{output}}(t)$ are normalized by their energy, respectively. The fidelity F is the maximum integration by varying time delay τ. The linear operator $L[\bullet]$ operates on the input pulse $p_{\mathrm{source}}(t)$. Evidently, the template at the output of a receiving antenna may be $L[p_{\mathrm{source}}(t)]$ not the simple $p_{\mathrm{source}}(t)$ for maximum fidelity. The calculated fidelity F for the single-band scheme and different operators $L[\bullet]$ are tabulated in Table I. Points can readily be observed from Table I. First, the waveforms of the received pulses are not identical with those of source pulses, especially for narrow-band antenna systems. Second, using sinusoidal templates, the fidelity F for the narrow-band antenna system is much higher than that for the broad-band one. This suggests that the spectrum of the received pulse is much narrower than that of source pulse after the antenna system with narrow bandpass filtering function. Third, using optimal Rayleigh's templates, the fidelity F can be increased greatly up to more than 0.9. The order $n > 1$ of the Rayleigh pulse suggests the differential functions of the antenna system. For the broad-band antenna system, the order is just four for

TABLE I
CALCULATED FIDELITY FOR THE PULSES IN THE SINGLE-BAND SCHEME

Antenna system	Source $p_{source}(t)$ with σ, ns	F for Template $p_{source}(t)$	F/ω, GHz for Template $\sin(\omega t)$	Template nth-order Rayleigh pulse		
				F	order, n	σ, ns
narrowband	30	0.74	0.80/6.16	0.89	6	83
	45	0.77	0.83/5.82	0.95	7	99
	80	0.58	0.88/5.25	0.99	12	149
broadband	30	0.70	0.62/3.86	0.94	4	78
	45	0.81	0.72/3.73	0.93	4	91
	80	0.87	0.87/3.21	0.95	4	129

all the three pulses. However, the order n for the narrow-band antenna system is larger than those for the broad-band antenna system and increases as the pulse becomes wider or the ratio of $L/\sigma c$ less.

V. CONCLUSION

This paper has presented the key considerations for source pulses and transmitting/receiving antenna systems for UWB radio systems in both single-band and multiband schemes. The studies have been carried out by means of the simulations in both time and frequency domains. Owing to the unique features of UWB radio systems, it is suggested to consider transmitting and receiving antennas as a system not single unit in the design. The special considerations for the source pulses and antennas have been suggested as follows.

1) The radiation levels of UWB signals must comply with the emission limit masks. The emission characteristics can be exactly described by a radiation transfer function. The investigation has demonstrated that for a multiband scheme properly selecting the envelope of modulated source pulses can effectively control the spectrum shaping of radiated signals. For a single-band scheme, there are at least three ways to shape the spectra of radiated signals. The first is to select the source pulses with spectrum shaping conforming to the emission limits mask. The second is to use RF filters to tailor the spectrum shaping of radiated signals. The last is to make use of the filtering function of transmitting antennas.
2) The antenna system should efficiently transmit and receive the signals. The transmission and reception performance of the antenna system can be mathematically described by a system transfer function. The investigation have manifested that within the UWB band the magnitude of the transfer function should be invariable or flat and the phase of the transfer function should be linear or the group delay is a constant. The transfer function with flat magnitude and linear phase frequency response has little distortion of the signals, which is conducive to the signal quality of the system.

It should be noted that other conventional antenna parameters, such as polarization and orientation should also be considered in the antenna design although this paper just highlights the special points for antenna systems for UWB radio systems.

REFERENCES

[1] Tektronix, Inc., Beaverton, OR, 97005, Instruction Manual: Type S-2 Sampling Head, 1968.
[2] G. F. Ross, "Transmission and Reception System for Generating and Receiving Base-Band Duration Pulse Signals for Short Base-Band Pulse Communication System," U.S. Patent 3 728 632, Apr. 17, 1973.
[3] C. L. Bennett and G. F. Ross, "Time-domain electromagnetics and its applications," *Proc. IEEE*, vol. 66, no. 3, pp. 299–318, 1978.
[4] H. F. Harmuth, *Nonsinusoidal Waves for Radar and Radio Communication*. New York: Academic, 1981.
[5] L. Carin and L. B. Felsen, *Ultra-Wideband Short-Pulse Electromagnetics*. New York: Plenum, 1995, vol. 2.
[6] M. Z. Win, R. A. Scholtz, and M. A. Barnes, "Ultra-wide bandwidth signal propagation for indoor wireless communications," in *Proc. IEEE Int. Conf. Commun.*, vol. 1, June 1997, pp. 56–60.
[7] R. J. Cramer, R. A. Scholtz, and M. Z. Win, "Evaluation of an ultra-wide-band propagation channel," *IEEE Trans. Antennas Propagat.*, vol. 50, pp. 561–570, May 2002.
[8] M. Welborn and J. McCorkle, "The importance of fractional bandwidth in ultra-wideband pulse design," in *IEEE Int. Conf. Commun. (ICC2002)*, vol. 2, 2002, pp. 753–757.
[9] M. Z. Win and R. A. Scholtz, "On the robustness of ultra-wide bandwidth signals in dense multipath environments," *IEEE Commun. Lett.*, vol. 2, pp. 51–53, Feb. 1998.
[10] D. Lamensdorf and L. Susman, "Baseband-pulse-antenna techniques," *IEEE Antennas Propagat. Mag.*, vol. 36, pp. 20–30, Feb. 1994.
[11] G. F. Ross, "A time domain criterion for the design of wideband radiating elements," *IEEE Trans. Antennas Propagat.*, vol. AP-16, no. 3, p. 355, 1968.
[12] A. Shlivinski, E. Heyman, and R. Kastner, "Antenna characterization in the time domain," *IEEE Trans. Antennas Propagat.*, vol. 45, pp. 1140–1149, July 1997.
[13] D. M. Pozar, "Waveform optimizations for ultra-wideband radio systems," *IEEE Trans. Antennas Propagat.*, vol. 51, pp. 2335–2345, Sept. 2003.
[14] H. J. Schmitt, C. W. Harrison Jr., and C. S. Williams Jr., "Calculated and experimental response of thin cylindrical antenna to pulse excitation," *IEEE Trans. Antennas Propagat.*, vol. 14, pp. 120–127, Mar. 1966.
[15] R. J. Palciauskas and R. E. Beam, "Transient fields of thin cylindrical antennas," *IEEE Trans. Antennas Propagat.*, vol. 18, pp. 276–278, Mar. 1970.
[16] D. M. Pozar, R. E. McIntosh, and S. G. Walker, "The optimum feed voltage for a dipole antenna for pulse radiation," *IEEE Trans. Antennas Propagat.*, vol. 31, pp. 563–569, July 1983.
[17] D. M. Pozar, D. H. Schaubert, and R. E. McIntosh, "The optimum transient radiation from an arbitrary antenna," *IEEE Trans. Antennas Propagat.*, vol. 32, pp. 633–640, June 1984.
[18] M. Onder and M. Kuzuoglu, "Optimal control of the feed voltage of a dipole antenna," *IEEE Trans. Antennas Propagat.*, vol. 40, pp. 414–421, Apr. 1992.
[19] J. Wang, L. Jen, and S. Jian, "Optimization of the dipole shapes for maximum peak values of the radiation pulse," in *Proc. IEEE Int. Antennas Propagat. Symp. Dig.*, vol. 1, July 1997, pp. 526–529.

[20] Z. N. Chen, X. H. Wu, N. Yang, and M. Y. W. Chia, "Design considerations for antennas in UWB wireless communication systems," in *Proc. IEEE Int. Symp. Antennas Propagation*, vol. 1, Columbus, OH, June 22–27, 2003, pp. 822–825.
[21] G. S. Smith, "On the interpretation for radiation from simple current distributions," *IEEE Antennas Propagat. Mag.*, vol. 40, pp. 9–14, June 1998.
[22] Z. N. Chen, X. H. Wu, and N. Yang, "Broadband planar monopoles for UWB radio systems," in *Proc. IEEE Asia-Pacific Microwave Conf.*, Seoul, Korea, Nov. 4–7, 2003.
[23] T. W. Hertel and G. S. Smith, "On the dispersive properties of the concial spiral antenna and its use for pulsed radiation," *IEEE Trans. Antennas Propagat.*, vol. 51, pp. 1426–1433, July 2003.

Zhi Ning Chen (M'99) was born in China. He received the Ph.D. degree in electrical engineering from the Institute of Communications Engineering (ICE), Nanjing, China, in 1993 and a second Ph.D degree from the University of Tsukuba, Tsukuba, Japan, in 2003.

From 1988 to 1995, he was with the ICE where he was appointed Teaching Assistant, Lecturer, and Associate Professor. After that, he worked at Southeast University (SEU), Nanjing, China, as a Postdoctoral Fellow and was then appointed an Associate Professor. From 1995 to 1997, he undertook research at the City University of Hong Kong, China, as a Research Assistant, Research Associate, Senior Research Associate, and Research Fellow. During 1997 to 1999, he worked at the University of Tsukuba, Japan, under a Fellowship awarded by Japan Society for Promotion of Science (JSPS). In 2000 and 2001, he visited SEU as a Visiting Scholar awarded by the Ministry of Education, China. In 2001, he visited the University of Tsukuba, under the Invitation Fellowship Program (senior level) of JSPS. In 1999, he joined the Centre for Wireless Communications (CWC) [later known as the Institute for Communications Research (ICR) and Institute for Infocomm Research $(\mathrm{I}^2\mathrm{R})$] as a Member of Technical Staff (MTS), Senior MTS, and Principal MTS, and currently a Lead Scientist and a Manager for the Department of Radio Systems. He is concurrently teaching and supervising postgraduate students at the National University of Singapore (NUS) as an Adjunct Associate Professor. From 2000 to 2004, he managed a research project on small and multiband antennas during. Since 1990, he has authored and coauthored over 120 technical papers in international journals and at conference proceedings. One of his patents has been granted and four are pending. His main research interests are applied computational electromagnetics, and antenna theory and designs. Currently, his research is focused on small, broad-band, lightweight antennas for wireless systems and ultrawide-band (UWB) radio systems, and metamaterials.

Dr. Chen was a Member of the Technical Program Committee and Organizer/Chair of the UWB Technology Workshop at the IEEE Radio and Wireless Conference in 2003 and 2004. He organized and Chaired a special session on Antennas for UWB Wireless Communication Systems at the IEEE International Symposium on Antennas and Propagation and the IEEE Asia and Pacific Microwave Conference, both in 2003.

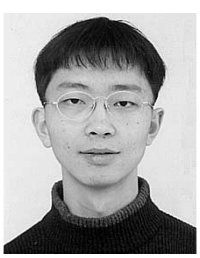

Xuan Hui Wu (S'03) was born in Hangzhou, Zhejiang Province, China, in January 1979. He received the B.Eng. degree from the Department of Information Science & Electronic Engineering (ISEE), Zhejiang University, Zhejiang Province, China, in 2001. Currently, he is working toward the M.Eng. degree in the Department of Electrical and Computer Engineering, National University of Singapore.

From November 2000 to November 2001, he worked as a part-time Research Assistant in the State Key Laboratory Computer Aided Design and Computer Graphics, Zhejiang University. From November 2001 to July 2002, he was a full-time Software Engineer at JQT Inc., Hangzhou, China. In July 2002, he joined the Institute for Infocomm Research $(\mathrm{I}^2\mathrm{R})$, Agency of Science Technology And Research, Singapore, as a Research Graduate Student. He has published ten papers in international journals and conferences. His current research interests include ultrawide-band radio systems and computational electromagnetics.

Hui Feng Li (S'03) was born in Shandong Province, China, in March 1980. He received the B.Eng. degree in electrical engineering from Shanghai Jiao Tong University, China, in 2002. He is currently working toward the M.Eng. degree in the Department of Electrical and Computer Engineering, National University of Singapore.

He is a Research Student with the Institute for Infocomm Research $(\mathrm{I}^2\mathrm{R})$, Agency of Science Technology And Research (ASTAR), Singapore. His current research interests include computational electromagnetics, optimization method, and ultrawide-band radio systems.

Ning Yang was born in Taixin, Jiangsu Province, China, in December 1976. He received the B.E.E.E. degree from the Radio Engineering Department, Southeast University, Nanjing, China, where he is currently working toward the Ph.D degree.

In 1998, he worked as a Graduate Student at the State Key Laboratory of Millimeter Waves, Southeast University. Since 1991, he has been with the Center for Wireless Communications (CWC), Singapore, as a Visiting Student where he was appointed an Associate Scientist by the Institute for Infocomm Research $(\mathrm{I}^2\mathrm{R})$, Agency of Science Technology And Research (ASTAR), Singapore. He has published 15 papers in international journals and conferences. His main research interests include ultrawide-band radio systems, applications of electromagnetic band-gap structures in microwave circuits, small- and wide-band printed antennas, and radio frequency identification antennas.

Michael Yan Wah Chia (M'90) was born in Singapore. He received the B.Sc. (1st Class Honors) and Ph.D. degrees from Loughborough University, Leicestershire, U.K., in 1990 and 1993, respectively.

In 1994, he joined the Center for Wireless Communications (CWC), Singapore, as a Member of Technical Staff (MTS), and was promoted to Senior MTS, Principal MTS, and finally Senior Principal MTS. He was also holding the appointment as Division Director of Radio Division. In 1999, he started the ultrawide-band (UWB) work at CWC, which later merged into the Institute for Infocomm Research $(\mathrm{I}^2\mathrm{R})$. He is the Division Director of Communications and Devices Division (which consists of five Departments) at the Institute for Infocomm Research, Agency of Science Technology And Research (ASTAR), Singapore. Concurrently, he has been appointed as an Adjunct Associate Professor at the National University of Singapore. Externally, he has also served in the Public Service Funding Panel of ASTAR-2002, Radio Standard Committee, and UWB task force Committee of the Infocomm Development Authority (IDA) of Singapore. He is also a Member of the Technical Program Committee for the International Workshop on UWB System (IWUWBS 2003), Finland. Since 2002, he has been listed in Marquis's *Who's Who in Engineering*. He has published 28 international journal papers and 50 international conference papers. He has 10 patents, both filed and granted, some of which have been commercialized and licensed to companies. His main research interests are UWB systems, antenna, transceiver, radio over fiber, RFIC, linearization, and communication and radar system architecture.

Dr. Chia was awarded an Overseas Research Studentship (ORS) and British Aerospace Studentship from the U.K.